BIOCHEMISTRY
including biophysical chemistry & molecular biology

Article

pubs.acs.org/biochemistry

Mechanism of Inhibition of GluA2 AMPA Receptor Channel Opening by 2,3-Benzodiazepine Derivatives: Functional Consequences of Replacing a 7,8-Methylenedioxy with a 7,8-Ethylenedioxy Moiety

Mohammad S. Qneibi,[†] Nicola Micale,[‡] Silvana Grasso,[‡] and Li Niu*[,†]

[†]Department of Chemistry and Center for Neuroscience Research, University at Albany, SUNY, Albany, New York 12222, United States
[‡]Dipartimento Farmaco-Chimico, Università di Messina, viale Annunziata, 98168 Messina, Italy

Supporting Information

ABSTRACT: 2,3-Benzodiazepine (2,3-BDZ) compounds are a group of AMPA receptor inhibitors and are drug candidates for treating neurological diseases involving excessive AMPA receptor activity. We investigated the mechanism by which GluA2Q$_{flip}$ receptor channel opening is inhibited by two 2,3-BDZ derivatives, i.e., 1-(4-aminophenyl)-3,5-dihydro-7,8-ethylenedioxy-4*H*-2,3-benzodiazepin-4-one (2,3-BDZ-11-2) and its 1-(4-amino-3-chlorophenyl) analogue (2,3-BDZ-11-4). Both compounds have a 7,8-ethylenedioxy moiety instead of the 7,8-methylenedioxy feature present in the structure of GYKI 52466, the prototypic 2,3-BDZ compound. Using a laser-pulse photolysis approach with a time resolution of ~60 μs and a rapid solution flow technique, we characterized the effect of the two compounds on the channel opening process of the homomeric GluA2Q$_{flip}$ receptor. We found that both 2,3-BDZ-11-2 and 2,3-BDZ-11-4 are noncompetitive inhibitors with specificity for the closed-channel conformation of the GluA2Q$_{flip}$ receptor. However, 2,3-BDZ-11-4 is ~10-fold stronger, defined by its inhibition constant for the closed-channel conformation (i.e., K_I = 2 μM), than 2,3-BDZ-11-2. From double-inhibitor experiments, we determined that both compounds bind to the same site, but this site is different from two other known, noncompetitive binding sites on the GluA2Q$_{flip}$ receptor previously reported. Our results provide both mechanistic clues to improve our understanding of AMPA receptor regulation and a structure−activity relationship for designing more potent 2,3-BDZ compounds with predictable properties for this new noncompetitive site.

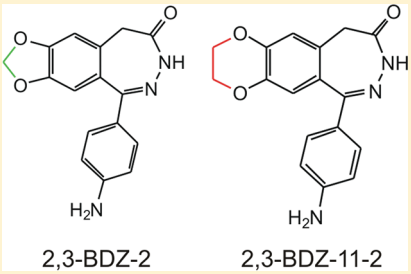

One of the most salient reasons for characterizing the mechanism of action of a series of structurally related regulatory molecules is to find "atomic descriptors" and to use them to design new compounds with predictable properties. In a structural sense, an atomic descriptor can be correlated to a unique position on an existing structure; for example, a single-atom substitution or addition at a particular position leads to a dramatic change in its function, such as a change in the binding site on the same molecular target. Consequently, one can develop new analogues to find new binding sites and to achieve more quantitative control of the target activity. As the fourth in a series of mechanistic studies designed to establish a more quantitative structure−activity relationship for 2,3-BDZ compounds, we herein describe the functional consequence of replacing a 7,8-methylenedioxy with a 7,8-ethylenedioxy moiety on the 2,3-benzodiazepine (2,3-BDZ) structure, represented most prominently by GYKI 52466 [i.e., 1-(4-aminophenyl)-4-methyl-7,8-methylenedioxy-5*H*-2,3-benzodiazepine].[1] GYKI 52466 is the prototypic 2,3-BDZ compound, based on which hundreds of derivatives have been synthesized.[2]

2,3-BDZ compounds are supposedly antagonists of the α-amino-3-hydroxy-5-methyl-4-isoxazolepropionic acid (AMPA) subtype of glutamate ion-channel receptors.[2−4] AMPA receptors mediate the majority of fast excitatory synaptic transmission in the central nervous system and are critically involved in neuronal development and brain activities, such as learning and memory.[5,6] Excessive activation of AMPA receptors is implicated in some neurological diseases, such as ischemia, epilepsy, and amyotrophic lateral sclerosis.[7] Therefore, antagonists of AMPA receptors are drug candidates for the treatment of such neurological diseases.[2,8] In fact, 2,3-BDZ compounds exhibit desirable anticonvulsant and neuroprotective properties in cellular and animal models.[9] To date, however, the mechanism of action of these compounds on AMPA receptors is not well understood, and a quantitative structure−activity relationship has not yet been established. These deficiencies are mainly attributed to the fact that an AMPA receptor opens its channel on the microsecond time domain but desensitizes on the millisecond time scale.[10] Previous studies of 2,3-BDZ compounds have not been conducted on the time scale in which the receptors are in the functional state. Consequently, it has not been possible to design 2,3-BDZ derivatives with predictable properties relevant to the time scale of the receptor function.

To characterize the functional consequence of replacing a 7,8-methylenedioxy with a 7,8-ethylenedioxy moiety on the 2,3-benzodiazepine structure, we focus on two 2,3-BDZ compounds, i.e., 1-(4-aminophenyl)-3,5-dihydro-7,8-ethylenedioxy-4*H*-2,3-benzodiazepin-4-one (2,3-BDZ-11-2) and its analogue

Received: November 28, 2011
Revised: January 30, 2012
Published: January 31, 2012

1-(4-amino-3-chlorophenyl)-3,5-dihydro-7,8-ethylenedioxy-4*H*-2,3-benzodiazepin-4-one (2,3-BDZ-11-4)[3,4] (Figure 1). 2,3-BDZ-11-2

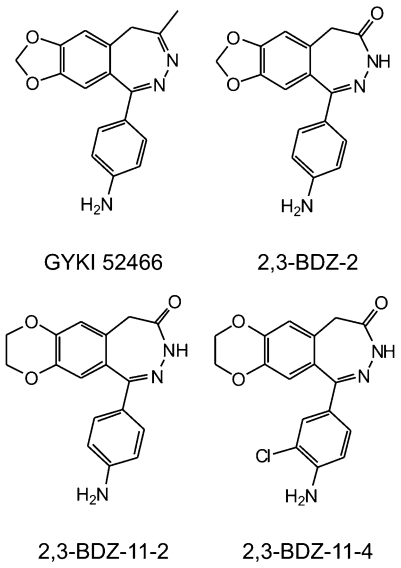

Figure 1. Chemical structures of GYKI 52466, 2,3-BDZ-2, 2,3-BDZ-11-2, and 2,3-BDZ-11-4. Their chemical names are given in the list of abbreviations and in the text.

and 2,3-BDZ-11-4 are more similar to 2,3-BDZ-2 [i.e., 1-(4-aminophenyl)-3,5-dihydro-7,8-methylenedioxy-4*H*-2,3-benzodiazepin-4-one][11] because they all have a carbonyl group at C-4 of the diazepine ring, whereas GYKI 52466 has a C-4 methyl group (Figure 1). However, in both 2,3-BDZ-11-2 and 2,3-BDZ-11-4, the 7,8-methylenedioxy feature, as in 2,3-BDZ-2, is replaced with a 7,8-ethylenedioxy moiety. Compared with 2,3-BDZ-11-2, 2,3-BDZ-11-4 contains an additional chlorine atom at C-3 of the aminophenyl ring (Figure 1).

Given these structural differences, we asked the following questions. What is the mechanism by which GluA2Q$_{flip}$ channel opening is inhibited by 2,3-BDZ-11-2 and 2,3-BDZ-11-4? Does the ring enlargement in 2,3-BDZ-11-2 at the 7,8-position change its potency and binding site with respect to 2,3-BDZ-2? What is the functional consequence of adding a chlorine atom at the C-3 position of the aminophenyl ring? Answers to these questions will provide a quantitative understanding of the functional consequences of these structural changes. To investigate these questions, we used a laser-pulse photolysis technique, together with a photolabile precursor of glutamate or caged glutamate, which provides a time resolution of ~60 μs.[10] This technique is suitable for measuring the rate of AMPA receptor channel opening and therefore allows us to elucidate the mechanism of inhibition for these compounds without the complication of channel desensitization that occurs on the millisecond time scale.[11−13] Furthermore, we chose to study these compounds with a homomeric GluA2Q$_{flip}$ channel, because the unedited isoform of GluA2 or GluA2Q is abnormally expressed in some neurological disorders.[14] Among the four AMPA receptor subunits, GluA2 is the one that controls the Ca^{2+} permeability of native AMPA receptor assemblies,[15] and an intracellular Ca^{2+} overload through Ca^{2+}-permeable AMPA receptor channels leads to neuronal death.[16]

EXPERIMENTAL PROCEDURES

Receptor Expression and Cell Culture. Human embryonic kidney 293S (HEK-293S) cells were cultured in Dulbecco's modified Eagle's medium supplemented with 10% fetal bovine serum at 37 °C in a 5% CO_2-humidified incubator.[17] HEK-293S cells were cotransfected to express GluA2Q$_{flip}$, together with the green fluorescent protein:large T-antigen:plasmid DNA weight ratio of 2:1:10.[18] The GluA2Q$_{flip}$ plasmid used for transfection was ~5−10 μg/35 mm Petri dish.[11] The cells were used for recording 48 h after transfection.

Whole-Cell Current Recording. Glutamate was used as the agonist in this study. Briefly, the resulting whole-cell current response was recorded using an Axopatch-200B amplifier at cutoff frequency of 2−20 kHz by a four-pole low-pass Bessel filter and acquired at a 5−50 kHz sampling frequency using a Digidata 1322A digitizer (Molecular Devices Corp.).[17] All recordings were collected at −60 mV, pH 7.4, and 25 °C. The electrode used for whole-cell recording was made from glass capillary and then fire polished.[17] The electrode was filled with an internal solution containing 110 mM CsF, 30 mM CsCl, 4 mM NaCl, 0.5 mM $CaCl_2$, 5 mM EGTA, and 10 mM HEPES (pH 7.4, adjusted with CsOH). The extracellular bath buffer contained 150 mM NaCl, 3 mM KCl, 1 mM $CaCl_2$, 1 mM $MgCl_2$, and 10 mM HEPES (pH 7.4, adjusted with NaOH). pCLAMP 8 was used for data collection.

Laser-Pulse Photolysis Measurement. A laser-pulse photolysis technique was used to liberate free glutamate surrounding a cell on a microsecond time scale from photolysis of 4-methoxy-7-nitroindolinyl-caged-L-glutamate.[13,19] The caged glutamate was applied to an HEK-293S cell suspended in the extracellular solution by a flow device.[20] The cell was equilibrated with the caged glutamate for at least 250 ms before it was irradiated with a 355 nm, 8 ns laser pulse. A single laser pulse of 200−1000 μJ was generated by a pulsed Q-switched Nd:YAG laser and then coupled into a fiber optic.[13] To calibrate the concentration of the photolytically released glutamate, we applied two free glutamate solutions with known concentrations to the same cell before and after a laser flash. The current amplitudes obtained from this calibration were compared with the amplitude from laser photolysis, with reference to the dose−response relation.

Measurement of the Channel Opening Rate Constant (k_{op}) and Channel Closing Rate Constant (k_{cl}). Using the laser-pulse photolysis technique combined with whole-cell recording, we determined the observed channel opening rate constant, k_{obs}, as a function of glutamate concentration, from which k_{op} and k_{cl} were calculated. In the laser-pulse photolysis measurement, the channel opening kinetic process followed a single-exponential rate expression, in eq 1, for ~95% of the rise time.

$$A_t = A_{max}(1 - e^{-k_{obs}t}) \quad (1)$$

where A_t represents the current amplitude at time t and A_{max} represents the maximal current amplitude. From eq 1, k_{obs} was calculated. Various k_{obs} values as a function of glutamate concentration can be described using a general mechanism of channel opening.[17]

$$R + nL \overset{K_1}{\rightleftharpoons} RL_n \underset{k_{cl}}{\overset{k_{op}}{\rightleftharpoons}} \overline{RL}_n$$

In the scheme described above, R stands for the active, unliganded form of the receptor, L the ligand or glutamate,

dx.doi.org/10.1021/bi2017552 | *Biochemistry* 2012, 51, 1787−1795

RL_n the closed channel forms with n ligand molecules bound, and $\overline{RL_n}$ the open-channel state. The number of glutamate molecules to bind to the receptor and to open its channel, n, can be from 1 to 4, assuming that a receptor is a tetrameric complex and each subunit has one glutamate binding site. However, our kinetic results of the channel opening rate process for AMPA receptors can be fully explained by the assumption that binding of two glutamate molecules per receptor complex is sufficient to open an AMPA receptor channel.[21] For simplicity and without contrary evidence, it is further assumed that glutamate binds with equal affinity or K_1, the intrinsic equilibrium dissociation constant, at all binding steps. As such, k_{obs} can be expressed by eq 2.[17]

$$k_{obs} = k_{cl} + k_{op}\left(\frac{L}{L + K_1}\right)^2 \quad (2)$$

In the derivation of eq 2, the ligand binding rate was assumed to be fast relative to the channel opening rate. This assumption was supported by the observation in which the channel opening rate process, represented by k_{obs}, was first-order in the absence[17] and presence of any inhibitors,[11−13] including those in this study.

Effect of an Inhibitor on k_{op} and k_{cl}. To elucidate the mechanism of inhibition by 2,3-BDZ-11-2 and 2,3-BDZ-11-4, we characterized the effect of each inhibitor on both k_{op} and k_{cl}.[11−13] If 2,3-BDZ-11-4, for instance, is an uncompetitive inhibitor or an open-channel blocker, it will inhibit only k_{cl} but not k_{op}.[11−13] If 2,3-BDZ-11-4 is a competitive inhibitor, it inhibits only k_{op} but not k_{cl}. Conversely, if 2,3-BDZ-11-4 is a noncompetitive inhibitor, it will inhibit both k_{cl} and k_{op} (see eq 3; this equation was used to analyze the effect of both 2,3-BDZ-11-2 and 2,3-BDZ-11-4 in Results and Discussion, as both turned out to be noncompetitive inhibitors).

To measure the effect of each inhibitor on k_{cl} and k_{op}, we varied the ligand (i.e., glutamate) concentration. This is because k_{obs} is a function of ligand concentration, and the magnitude of k_{obs} is contributed by both k_{cl} and k_{op} terms (eq 2).[10−13] Therefore, if the ligand concentration is low (i.e., $L \ll K_1$), eq 2 is reduced to $k_{obs} \approx k_{cl}$. Similarly, in the presence of an inhibitor, eq 3 is reduced to $k_{obs} \approx k_{cl}'$. In other words, the effect of an inhibitor on k_{cl} and its inhibition constant ($\overline{K_I}$) for the open-channel state are determined with the use of eq 4 (here eq 4 is expressed as the linear form to yield $\overline{K_I}$ by linear regression). At a higher ligand concentration, where $k_{obs} > k_{cl}$, the k_{op} value can be determined by the difference between k_{obs} and k_{cl} or by rearranging (eq 2) such that $k_{obs} - k_{cl} = k_{op}[L/(L + K_1)]^2$. Similarly, the effect of an inhibitor on k_{op} and the inhibition constant (K_I) for the closed-channel state (here the closed-channel state refers to the unliganded, singly and doubly liganded forms, assuming $n = 2$) can be determined with the use of eq 5.

$$k_{obs} = k_{cl}\left(\frac{\overline{K_I}}{\overline{K_I} + I}\right) + k_{op}\left(\frac{L}{L + K_1}\right)^2\left(\frac{K_I}{K_I + I}\right) \quad (3)$$

$$\frac{1}{k_{obs}} = \frac{1}{k_{cl}} + \frac{1}{k_{cl}}\frac{I}{\overline{K_I}} \quad (4)$$

$$(k_{obs} - k_{cl}')^{-1} = \left[\frac{k_{op}L^2}{(L + K_1)^2}\right]^{-1}\left(1 + \frac{I}{K_I}\right) \quad (5)$$

We previously established the criteria by which k_{cl} can be determined from the measurement of k_{obs}.[10,11,17] For GluA2Q$_{flip}$, k_{cl} is numerically equal to the k_{obs} value obtained at 100 μM glutamate, which corresponds to ~4% of the fraction of the open-channel form.[10,11,17] As such, the effect of 2,3-BDZ-11-2 or 2,3-BDZ-11-4 on k_{cl} was determined at this glutamate concentration.[11] The effect on k_{op} was determined at a glutamate concentration of 300 μM.[11] At this concentration, the difference between k_{op} and k_{cl} could be detected while the energy used for laser photolysis was still well tolerated by the cell.

Effect of an Inhibitor on Current Amplitude. The effect of 2,3-BDZ-11-2 or 2,3-BDZ-11-4 on the whole-cell current amplitude (A) was measured to calculate independently an inhibition constant. Specifically, we used a low glutamate concentration (i.e., $L \ll K_1$), at which most receptors were in the closed-channel state, to determine the inhibition constant for the closed-channel state (eqs 6a and 6b). To determine the inhibition constant for the open-channel state, we used a saturating ligand concentration ($L \gg K_1$), at which most receptors were in the open-channel state.[11−13] For GluA2Q$_{flip}$, we chose 100 μM and 3 mM for the low and high glutamate concentrations, respectively. These concentrations correspond to ~4 and ~95% of the open-channel form, respectively.[11−13]

$$\frac{A}{A_I} = 1 + I\frac{(\overline{RL_2})_O}{K_I} \quad (6a)$$

where $(\overline{RL_2})_O$ represents the fraction of the open-channel state and is proportional to the current amplitude. In eq 6b, this fraction is expressed as a function of the fraction of all receptor forms, and Φ^{-1} is the channel opening equilibrium constant.

$$(\overline{RL}_2)_O = \frac{\overline{RL}_2}{R + RL + RL_2 + \overline{RL_2}} = \frac{L^2}{L^2(1 + \Phi) + 2K_1L\Phi + K_1{}^2\Phi} \quad (6b)$$

Experimentally, a flow device was used to apply glutamate at a known concentration in the absence and presence of an inhibitor.[11] The time resolution of the flow device, determined by the rise time of the whole-cell current response (10−90%) to saturating glutamate concentrations, was 1.0 ± 0.2 ms.[11−13] For data analysis, the observed amplitude of the whole-cell current was corrected for receptor desensitization.[20] Furthermore, full inhibition by 2,3-BDZ-11-2 or 2,3-BDZ-11-4 was achieved only by preincubating the GluA2Q$_{flip}$ receptor with either inhibitor for at least 6 s, similar to the results for other 2,3-BDZ compounds we studied previously.[11−13]

Double-Inhibitor Experiment To Assess the Binding Site. To investigate whether two inhibitors bound to the same site or to two different sites on GluA2Q$_{flip}$, we examined the effect of two inhibitors on the whole-cell current amplitude (eqs 7 and 8) and compared that with the effect of just one inhibitor (eq 6).[11−13] Specifically, the amplitude was used, similar to eq 6, to plot $A/A_{I,P}$ versus one inhibitor concentration. Here, one inhibitor is represented as I in molar concentration and the other is P. If binding of one inhibitor excludes the binding of the other (i.e., in the one-site model, A·I and A·P

dx.doi.org/10.1021/bi2017552 | Biochemistry 2012, 51, 1787−1795

complexes are allowed but not the A·I·P complex), the ratio of the current amplitude is given in eq 7.

$$\frac{A}{A_{I,P}} = 1 + \frac{P}{K_P} + \frac{I}{K_I} \quad (7)$$

Conversely, for a two-site model in which there are two sites for I and P separately and binding of one inhibitor is independent of the binding of the other (i.e., A·I, A·P, and A·I·P complexes are all allowed), the ratio of the current amplitude is given in eq 8.

$$\frac{A}{A_{I,P}} = 1 + \frac{P}{K_P} + \left(1 + \frac{P}{K_P}\right)\frac{I}{K_I} \quad (8)$$

In the double-inhibitor experiment, the concentration of one inhibitor was kept constant while the concentration of the other was varied. An apparent inhibition constant obtained from the two-inhibitor experiment [or the slope of the $A/A_{I,P}$ plot (see eqs 7 and 8)] was compared to that obtained from the one-inhibitor experiment [or the slope of the A/A_I plot (see eqs 6a and 6b)]. All other conditions were the same as those described for measuring the effect of an inhibitor on the current amplitude.

Origin 7 was used for both linear and nonlinear regression analysis in this study. Unless otherwise noted, each data point shown in a plot was an average of at least three measurements collected from at least three cells. The error reported refers to the standard deviation of a fit.

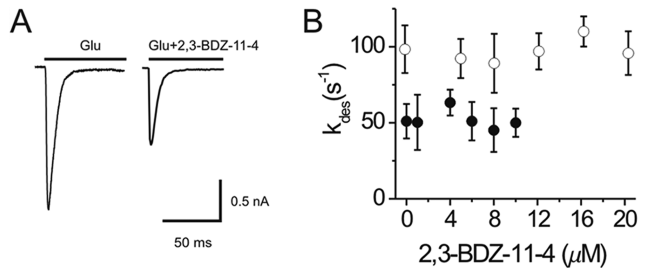

Figure 2. (A) Pair of representative whole-cell current traces from GluA2Q$_{flip}$ channels expressed in HEK-293 cells in the absence (left) and presence (right) of 2,3-BDZ-11-4. The whole-cell current recording was conducted at −60 mV, pH 7.4, and 22 °C. The concentrations of glutamate and inhibitor were 3 mM and 10 μM, respectively. (B) Effect of 2,3-BDZ-11-4 on the channel desensitization rate constants determined at 100 μM (●) and 3 mM glutamate (○) (the same data for 2,3-BDZ-11-2 are shown in Figure S1 of the Supporting Information).

RESULTS AND DISCUSSION

2,3-BDZ-11-2 and 2,3-BDZ-11-4 Inhibited the Channel Opening Rate of GluA2Q$_{flip}$. 2,3-BDZ-11-2 and 2,3-BDZ-11-4 inhibited GluA2Q$_{flip}$ channel activity, shown in a reduction of whole-cell current (Figure 2A). Because neither 2,3-BDZ-11-4 (Figure 2B) nor 2,3-BDZ-11-2 (Figure S1 of the Supporting Information) affected the rate of channel desensitization at various concentrations of glutamate and inhibitors, we focused our investigation on the effect of these two compounds on the rate of channel opening of GluA2Q$_{flip}$, using the laser-pulse photolysis technique. Figure 3A shows a representative whole-cell current trace generated by photolysis of the caged glutamate. In the presence of 2,3-BDZ-11-4, for example, the rise of the whole-cell current was slowed and the amplitude reduced, indicating that 2,3-BDZ-11-4 inhibited the opening of the GluA2Q$_{flip}$ channel. In the absence or presence of an inhibitor, the channel opening rate could be described by a first-order rate process for more than 95% of the rising phase (Figure 3A). In fact, a single-exponential rate for the current rise was observed, without exception, for all inhibitor and glutamate concentrations in this study and previous studies of GluA2Q$_{flip}$.[11,17] These results therefore support the notion that the rate of the current rise in the laser-pulse photolysis measurement was representative of the channel opening rate rather than the ligand binding rate process.[11,17] The reduction of the rate of current rise was thus ascribed to the inhibition of channel opening by an inhibitor.

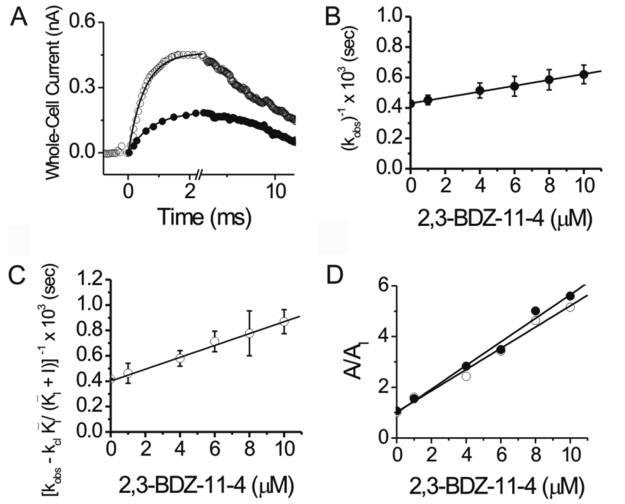

Figure 3. (A) In a laser-pulse photolysis experiment, 2,3-BDZ-11-4 inhibited both the rate and the amplitude of the whole-cell current rise reflecting the opening of the GluA2Q$_{flip}$ channel. The top trace is the control (k_{obs} = 2425 s^{-1}; A = 0.52 nA), and the bottom is for 4 μM 2,3-BDZ-11-4 (k_{obs} = 2274 s^{-1}; A = 0.24 nA). In both cases, the concentration of the photolytically released glutamate was estimated to be 300 μM. (B) Effect of 2,3-BDZ-11-4 on k_{cl} obtained at 100 μM glutamate and as a function of 2,3-BDZ-11-4 concentration. From this plot, a $\bar{K}_I$* of 24 ± 5.0 μM was obtained using eq 4. (C) Effect of 2,3-BDZ-11-4 on k_{op} obtained at 300 μM glutamate and as a function of 2,3-BDZ-11-4 concentration. From this plot, a K_I* of 9.0 ± 3.0 μM was determined using eq 5. The plots for the effect of 2,3-BDZ-11-2 on the channel opening rate constants are provided in Figure S2 of the Supporting Information. (D) Effect of 2,3-BDZ-11-4 on the amplitude of the whole-cell current in the absence and presence of 2,3-BDZ-11-4, determined from laser-pulse photolysis measurements. A K_I of 2.3 ± 0.2 μM was obtained from the plot of A/A_I values vs 2,3-BDZ-11-4 concentration for the closed-channel state (●; 100 μM glutamate). The K_I was determined to be 2.4 ± 1.0 μM at 300μM of photolytically released glutamate (○). Each data point shown in this plot was an average of at least three measurements collected from at least three cells.

We then characterized exclusively the effect of an inhibitor on k_{cl} and determined the inhibition constant for the open-channel form ($\bar{K}_I$*) at 100 μM glutamate, using eq 4.[10−13] Specifically, a $\bar{K}_I$* of 24 ± 5.0 μM for 2,3-BDZ-11-4 was determined for the open-channel state (Figure 3B), and a $\bar{K}_I$* of 43 ± 11 μM was determined for 2,3-BDZ-11-2 (Figure S2A of the Supporting Information). (Note that for clarity the data presented in the text are mostly for 2,3-BDZ-11-4, while the data for 2,3-BDZ-11-2 are presented in Supporting Information.

dx.doi.org/10.1021/bi2017552 | Biochemistry 2012, 51, 1787−1795

Table 1. Summary of the Inhibition Constants of 2,3-BDZ-11-4, 2,3-BDZ-11-2, 2,3-BDZ-2, and GYKI 52466, Obtained from Rate and Amplitude Measurements, for the Closed- and Open-Channel States of GluA2Q$_{flip}$

	rate measurement[a]		amplitude measurement			
inhibitor	K_I* (μM)[b,d] (closed channel)	$\overline{K_I}$* (μM)[b,e] (open channel)	K_I (μM)[b,d]	K_I (μM)[b,e]	K_I (μM)[c,d] (closed channel)	$\overline{K_I}$ (μM)[c,f] (open channel)
2,3-BDZ-11-4	9.0 ± 3.0	24 ± 5.0	2.3 ± 0.2	2.4 ± 1.0	2.0 ± 0.1	14 ± 0.4
2,3-BDZ-11-2	39 ± 9.0	43 ± 11	19 ± 1.0	24 ± 4.0	21 ± 0.1	33 ± 1.0
2,3-BDZ-2[g]	48 ± 5.0	194 ± 20	25 ± 1.0	23 ± 1.0	25 ± 1.0	7.0 ± 1.0
GYKI 52466[h]	61 ± 11	128 ± 30	15 ± 1.0	16 ± 1.0	14 ± 1.0	30 ± 2.0

[a]The constants obtained from rate measurements represent those in the first step of inhibition, as in Figure 5, whereas those obtained from the amplitude measurements represent the overall inhibition constants. [b]Laser-pulse photolysis measurement. [c]Flow measurement. [d]Measurements at 100 μM glutamate for the closed-channel state. [e]Measurements at ~300 μM glutamate. [f]Measurements at 3 mM glutamate. [g]From ref 11. [h]From ref 12.

Furthermore, 2,3-BDZ-11-4 and 2,3-BDZ-11-2 have an identical mechanism of action.) At a higher ligand concentration [i.e., 300 μM glutamate (see also Experimental Procedures)], the effect of an inhibitor on k_{op} was further determined. A K_I* of 9.0 ± 3.0 μM for the closed-channel state was obtained (eq 5) for 2,3-BDZ-11-4 (Figure 3C). Similarly, a K_I* of 39 ± 9.0 μM was obtained for 2,3-BDZ-11-2 (Figure S2B of the Supporting Information). These values are also summarized in Table 1.

Effect of 2,3-BDZ-11-2 and 2,3-BDZ-11-4 on the Amplitude of the Whole-Cell Current Determined by Laser-Pulse Photolysis Measurement. As shown in a laser-pulse photolysis measurement (Figure 3A), 2,3-BDZ-11-4 inhibited the time course of the current rise and concurrently the amplitude of the whole-cell current. From the amplitude of the whole-cell current in the absence and presence of 2,3-BDZ-11-4 (Figure 3D), a K_I of 2.3 ± 0.2 μM was obtained, using eqs 6a and 6b, at 100 μM glutamate for the closed-channel state. Similarly, a $\overline{K_I}$ of 2.4 ± 1.0 μM was estimated at 300 μM glutamate (Figure 3D). These inhibition constants obtained from the amplitude in the laser measurement are also summarized in Table 1.

However, inspection of the inhibition constants obtained from the rate (Figure 3B,C) and amplitude data (Figure 3D) from the same experiment (i.e., the laser-pulse photolysis measurement) for the same inhibitor (e.g., 2,3-BDZ-11-4) showed a clear discrepancy. For instance, a K_I* of 9.0 ± 3.0 μM for the closed-channel state of GluA2Q$_{flip}$ was obtained from the rate data for 2,3-BDZ-11-4 (i.e., the data in column 1 of Table 1), but a K_I of 2.3 ± 0.2 μM was obtained from the amplitude data (i.e., the data in column 3 of Table 1). For 2,3-BDZ-11-2, we observed a smaller but statistically significant difference in the inhibition constant determined from the amplitude data as compared with the rate data (Figure S3 of the Supporting Information and Table 1).

Effect of 2,3-BDZ-11-2 and 2,3-BDZ-11-4 on the Amplitude of the Whole-Cell Current from Flow Measurement. As described above, the rate and amplitude data from the laser-pulse photolysis experiment produced different inhibition constants. To investigate this difference, we used a solution flow technique with known concentrations of glutamate and measured the current amplitude. From the plot of A/A_I as a function of inhibitor concentration, we independently characterized the inhibition constant for each inhibitor. For 2,3-BDZ-11-4, a K_I of 2.0 ± 0.1 μM for the closed-channel state and a $\overline{K_I}$ of 14 ± 0.4 μM for the open-channel state (Figure 4) were determined. For 2,3-BDZ-11-2, a K_I of 21 ± 0.1 μM for the closed-channel state and a $\overline{K_I}$ of 33 ± 1.0 μM for the open-channel state were calculated (Figure S4 of the Supporting Information; all these values are also summarized in Table 1). By comparison, inhibition constants obtained from the amplitude data from both the flow and the laser experiments were the same. For instance, at the same glutamate concentration (i.e., either 100 or 300 μM), the K_I value for 2,3-BDZ-11-4 estimated from the amplitude data for the closed-channel state was 2.3 μM by the flow measurement and 2.0 μM by the laser experiment (Table 1). Therefore, the apparent discrepancy in inhibition constant between the rate and amplitude measurements was real (the difference will be discussed below in detail).

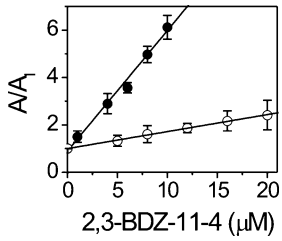

Figure 4. Inhibition constants of 2,3-BDZ-11-4 estimated from the amplitude of the whole-cell current through GluA2Q$_{flip}$ channels by the solution flow measurement. At 3 mM glutamate (○), a $\overline{K_I}$ of 14 ± 0.4 μM was obtained, corresponding to the inhibition constant for the open-channel state. Similarly, a K_I of 2.0 ± 0.1 μM was obtained for the closed-channel state at a glutamate concentration of 100 μM (●).

It should be pointed out that at 3 mM glutamate, where ~95% of the channels were in the open-channel state,[17] an inhibition constant was pertinent to the open-channel state of GluA2Q$_{flip}$ (see also eqs 6a and 6b). However, reaching 3 mM glutamate by laser-pulse photolysis of caged glutamate was not technically feasible in our experiment. Furthermore, an inhibition constant obtained from the amplitude data collected from the laser experiment at 300 μM glutamate (data in column 4) was closer to an inhibition constant obtained from 100 μM glutamate (data in either column 3 or 5), rather than to that for 3 mM glutamate (data in column 6). This result was anticipated, because the fraction of the open-channel form that corresponds to 300 μM glutamate is ~10%, which is closer to ~4% at 100 μM glutamate but far from ~93% at 3 mM glutamate or the maximal limit set by the channel opening probability for GluA2Q$_{flip}$.[17]

2,3-BDZ-11-2 or 2,3-BDZ-11-4 Inhibits Channel Opening by a Two-Step Process. As described above, the inhibition constants calculated from the amplitude data from both the laser-pulse photolysis and the flow measurements were in good agreement (Table 1). However, those constants were 2−4-fold smaller than the inhibition constants estimated from rate measurement (Table 1). In other words, as compared with the full inhibition or full antagonism observed from the amplitude measurement, the effect of an inhibitor on rate projected only

dx.doi.org/10.1021/bi2017552 | Biochemistry 2012, 51, 1787−1795

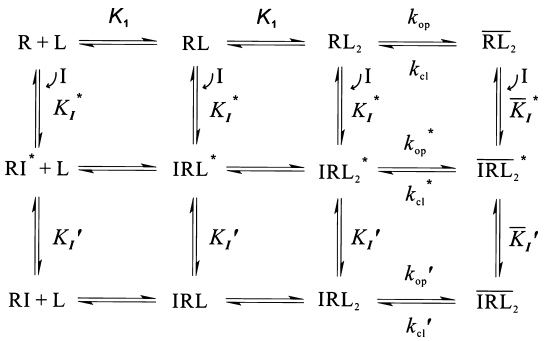

Figure 5. Minimal mechanism of inhibition of the GluA2Q$_{flip}$ receptor by 2,3-BDZ-11-2 and 2,3-BDZ-11-4. L represents ligand or glutamate, and the number of ligands that bind to and open the channel is assumed to be 2. R represents the active, unliganded form of the receptor, and I represents an inhibitor. For the sake of simplicity and without contrary evidence, it is assumed that glutamate binds with equal affinity or K_1, the intrinsic equilibrium dissociation constant, at all binding steps. An asterisk indicates those species in the intermediate state, i.e., loose receptor−inhibitor complexes, whereas those species bound with inhibitor but without an asterisk represent those in the final state of the receptor complexes. All species related to R, RL, and RL_2, including those bound with inhibitors, are in closed-channel states, whereas those related to $\overline{RL}_2$ refer to the open-channel state. Because the channel desensitization rate constant is unaffected by 2,3-BDZ-11-2 (Figure S1 of the Supporting Information) or 2,3-BDZ-11-4 (Figure 2B), the channel desensitization process is not included in this scheme or in our analysis.

partial inhibition or partial antagonism. This discrepancy can be ascribed to the mechanism of inhibition that we have proposed previously for other 2,3-BDZ inhibitors (Figure 5).[11−13] Specifically, the initial binding of 2,3-BDZ-11-4, for instance, to the receptor forms a loosely bound channel complex (e.g., $\overline{IRL}_2$*), and such a receptor−inhibitor complex is partially conducting, thereby resulting in only partial inhibition of receptor activity. Additional reduction of the current amplitude comes from the second step in which the receptor−inhibitor intermediate isomerizes rapidly into a more tightly bound complex (e.g., $\overline{IRL}_2$); such a complex is no longer conductive. This two-step inhibition process involving the formation of loose intermediates applies to both the closed-channel and open-channel states (Figure 5).

The mode of action of 2,3-BDZ-11-4 and 2,3-BDZ-11-2 can be explained by this mechanism of inhibition (Figure 5). First, in the laser-pulse photolysis measurement, the effect of an inhibitor on both the channel closing rate and the whole-cell amplitude was associated with a rapid channel opening process. Therefore, a stronger inhibition or a smaller K_I value calculated from the amplitude, which was an equilibrium measure, suggested that a larger value of the inhibition constant observed from the rate would have to reflect a fraction of the overall inhibition (e.g., the values in column 1 vs those in column 3 or column 5). Second, the partial inhibitory effect on the channel opening rate would reflect the first step in Figure 5 for the formation of an inhibitor−receptor complex; additional inhibition was thus generated from the second step in which the partially conducting inhibitor−receptor complex isomerizes into a totally inhibitory complex. Third, in the presence of 2,3-BDZ-11-4, for example, the rate of channel opening of the GluA2Q$_{flip}$ receptors was slow compared with the control (Figure 3A). A slower rate should reflect the first step involving the formation of the loose receptor−inhibitor intermediate; the second step, however, should be faster than the first step. If the rate of the second step were slow or comparable to that of the first step, full or virtually full inhibition would be expected in that the inhibition constants determined from the rate would be equal or nearly equal to those obtained from the amplitude data. A significant difference in rate is also consistent with the fact that over the entire concentration range for both glutamate and the inhibitors, only a single-exponential rise for the rate of channel opening was observed. Therefore, the effect of an inhibitor on the channel opening rate was analyzed adequately by use of the one-step process (eqs 4 and 5). That $1/k_{obs}$ increased linearly with an increasing inhibitor concentration (Figure 3B,C), as predicted (by eqs 4 and 5), for both the closed- and open-channel states, further supports the notion that the rate of the isomerization reaction would be faster than the first step. Consequently, $\overline{K_I}$* and K_I* values (Table 1) obtained from the rate measurement reflected partial inhibition of the open- and closed-channel states, respectively, by 2,3-BDZ-11-4 or 2,3-BDZ-11-2 in the first step (Figure 5).

The finding that 2,3-BDZ-11-4 and 2,3-BDZ-11-2 inhibited both k_{op} and k_{cl}, albeit partially, is consistent with a noncompetitive mechanism of inhibition for both inhibitors but inconsistent with either a competitive or an uncompetitive mechanism. By a competitive mode of action, 2,3-BDZ-11-4 would be expected to compete with glutamate for the same binding site; therefore, only the effect on k_{op}, but not on k_{cl}, would be expected. Consequently, there would be no $\overline{K_I}/(\overline{K_I} + I)$ term associated with k_{cl} in eq 3, and thus, $1/k_{obs}$ as in eq 4 would be independent of inhibitor concentration. By an uncompetitive mode of action, commonly known as open-channel blockade, 2,3-BDZ-11-4 would inhibit the open-channel state only. As such, only the effect on k_{cl}, but not that on k_{op}, would be expected. In this case, the $K_I/(K_I + I)$ term associated with k_{op} in eq 3 does not exist. As a result, the $k_{obs} - k_{cl}'$ term, as in eq 5, would not depend on inhibitor concentration.

2,3-BDZ-11-2 and 2,3-BDZ-11-4 Inhibited the Closed-Channel State More Strongly Than the Open-Channel State of the Flip and Flop Isoforms of GluA2. On the basis of the overall inhibition constants (Table 1), both 2,3-BDZ-11-2 and 2,3-BDZ-11-4 were selective for the closed-channel state of the GluA2Q$_{flip}$ channel [e.g., K_I of 2.0 ± 0.1 μM vs $\overline{K_I}$ of 14 ± 0.4 μM for 2,3-BDZ-11-4 (Figure 4)]. It is also worth noting that 2,3-BDZ-11-4 showed a comparable potency and selectivity for the flop variant of GluA2Q or GluA2Q$_{flop}$. GluA2Q$_{flop}$ is the alternatively spliced isoform of GluA2Q$_{flip}$, and the two isoforms differ by only eight amino acids.[22] However, the homomeric GluA2Q$_{flip}$ and GluA2Q$_{flop}$ channels have different kinetic properties such that the flop variant of GluA2 has the same k_{op} but a larger k_{cl} than the flip variant.[23] For this study, we used the flow technique and determined the overall inhibition constants for the closed-channel and open-channel states of both types of homomeric channels. We found that 2,3-BDZ-11-4 inhibited the GluA2Q$_{flop}$ receptors expressed in HEK-293 cells with a K_I of 2.4 ± 0.1 μM for the closed-channel state and a $\overline{K_I}$ of 19 ± 0.2 μM for the open-channel state (Figure 6). Furthermore, 2,3-BDZ-11-2 inhibited the GluA2Q$_{flop}$ receptors with a K_I of 25 ± 0.3 μM for the closed-channel state and a $\overline{K_I}$ of 33 ± 1.0 μM for the open-channel state (Figure S5 of the Supporting Information). These inhibition constants were comparable to those of GluA2Q$_{flip}$ (Table 1), suggesting that 2,3-BDZ-11-4 and 2,3-BDZ-11-2 were equally effective on

dx.doi.org/10.1021/bi2017552 | Biochemistry 2012, 51, 1787−1795

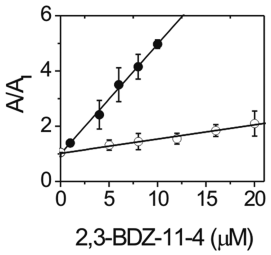

Figure 6. Inhibition constants of 2,3-BDZ-11-4 for the flop variant of GluA2Q (GluA2Q$_{flop}$). The constants were estimated from the amplitude of the whole-cell current in the absence and presence of 2,3-BDZ-11-4, collected from the flow measurement. A $\overline{K_I}$ of 19.0 ± 0.2 μM was obtained at 3 mM glutamate (○), which corresponds to the inhibition constant for the open-channel state. A K_I of 2.4 ± 0.1 μM was obtained at 100 μM glutamate (●), which corresponds to the closed-channel state.

GluA2Q$_{flop}$, and both were also selective for the closed-channel state of the GluA2Q$_{flop}$ channel.

2,3-BDZ-11-2 and 2,3-BDZ-11-4 Bind to the Same Site on the GluA2Q$_{flip}$ Receptor. Our results show that 2,3-BDZ-11-2 and 2,3-BDZ-11-4 are noncompetitive inhibitors, although 2,3-BDZ-11-4 is stronger than 2,3-BDZ-11-2. On the basis of the structural (Figure 1) and functional similarities between the two compounds, we asked whether they competed at the same noncompetitive site or bound to two different sites on the same receptor. The outcome would provide important insights into the structure−activity relationship of 2,3-BDZ derivatives. To address this question, we conducted a double-inhibitor experiment (see Experimental Procedures) in which 2,3-BDZ-11-2 and 2,3-BDZ-11-4 were used simultaneously to inhibit the GluA2Q$_{flip}$ receptor. The double-inhibition constant, K_I', was 1.8 ± 1.0 μM (Figure 7A), which was comparable to the K_I of 2.0 ± 0.1 μM for 2,3-BDZ-11-4 alone (Figure 4 and Table 1). This result suggested that the two inhibitors compete for the same noncompetitive site on GluA2Q$_{flip}$ receptors. If 2,3-BDZ-11-2 and 2,3-BDZ-11-4 bound to two different sites, a much stronger inhibition produced by the presence of two inhibitors would likely be observed in the same concentration range (Figure 7A, dashed line, simulated by eq 8).

We previously reported a unique noncompetitive binding site for 2,3-BDZ-2[11] and another site for GYKI 52466 (see Figure 1).[12,13] The molecular determinant of the two sites is thought to be the nature of the C-4 substitution on the diazepine ring. Specifically, the C-4 position of GYKI 52466 is a methyl group, whereas in 2,3-BDZ-2, it is a carbonyl group. Furthermore, GYKI 52466 is selective for the closed-channel state,[12,13] whereas 2,3-BDZ-2 prefers to inhibit the open-channel state of GluA2Q$_{flip}$.[11] Because 2,3-BDZ-11-2 and 2,3-BDZ-11-4 share the C-4 carbonyl feature with 2,3-BDZ-2 (Figure 1), it was assumed that they would compete with the 2,3-BDZ-2 binding site. However, double-inhibition experiments revealed that 2,3-BDZ-11-2 and 2,3-BDZ-11-4 did not bind to the 2,3-BDZ-2 site (Figure 7B) or to the GYKI 52466 site (Figure 7C); in both cases (Figure 7B,C), a much stronger inhibition was observed in the presence of either 2,3-BDZ-2 or GYKI 52466, together with 2,3-BDZ-11-2, compared to the inhibition by a predicted single site (the dashed line in panels B and C of Figure 7). These results suggested that the noncompetitive site where 2,3-BDZ-11-2 and 2,3-BDZ-11-4 bound was new or different from either of the two sites we reported previously.[11−13]

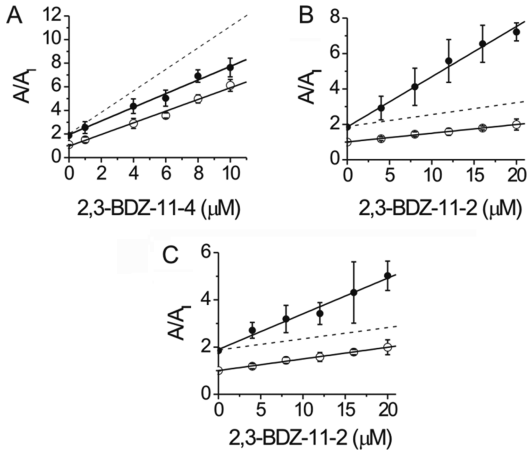

Figure 7. Double-inhibition experiment to characterize inhibitor binding sites. (A) 2,3-BDZ-11-2 and 2,3-BDZ-11-4 bind to the same site on GluA2Q$_{flip}$. In this experiment, the concentrations of 2,3-BDZ-11-2 and glutamate were fixed at 20 and 100 μM, respectively. From the amplitude data in the presence of both 2,3-BDZ-11-2 and 2,3-BDZ-11-4 (●), the double-inhibition constant, K_I', was determined to be 1.8 ± 1.0 μM (using eq 7), as compared with the K_I of 2.0 ± 0.1 μM for 2,3-BDZ-11-4 alone (○; Figure 4 and Table 1). The dashed line is the simulated result from eq 8, assuming that the two inhibitors bound to two different sites. (B) 2,3-BDZ-11-2 and 2,3-BDZ-2 do not bind to the same site on GluA2Q$_{flip}$. The concentrations of 2,3-BDZ-2 and glutamate were kept at 20 and 100 μM, respectively. The double-inhibition constant, K_I', was determined to be 10 ± 2.0 μM (●), as compared with a K_I of 21 ± 0.1 μM for 2,3-BDZ-11-2 alone (○; Figure S4 of the Supporting Information). The dashed line is the simulation based on eq 7, assuming that the two inhibitors bound to the same site. (C) 2,3-BDZ-11-2 and GYKI 52466 do not bind to the same site on GluA2Q$_{flip}$. In this experiment, the concentrations of GYKI 52466 and glutamate were fixed at 15 and 100 μM, respectively, while the concentration of 2,3-BDZ-11-2 was varied. The double-inhibition constant, K_I', was 14.0 ± 3.0 μM (●), compared with a K_I of 21 ± 0.1 μM for 2,3-BDZ-11-2 alone (○; Figure S4 of the Supporting Information). The dashed line represents the simulated A/A_1 values by using eq 7, assuming that the two inhibitors bound to the same site.

Effect of Replacing a 7,8-Methylenedioxy with a 7,8-Ethylenedioxy Moiety on Binding Sites of 2,3-BDZ Compounds. Structurally, 2,3-BDZ-11-2 is most similar to 2,3-BDZ-2 (Figure 1). The two compounds were synthesized[3,4] on the basis of the structure of GYKI 52466 (Figure 1).[24,25] To replace the 4-methyl group of GYKI 52466 with a carbonyl group to produce 2,3-BDZ-2, the double bond between N-3 and C-4 of the diazepine ring must be saturated (Figure 1). Thus, the structural difference between GYKI 52466 and 2,3-BDZ-2 is a replacement of the azomethine moiety with an ε-lactam moiety (alternatively, this structural change can be considered a replacement of the iminohydrazone moiety of GYKI 52466 by an iminohydrazide moiety, resulting in 2,3-BDZ-2). As we previously reported, such a replacement forces 2,3-BDZ-2 to bind to a new noncompetitive site on GluA2Q$_{flip}$.[11−13] In other words, if a methyl group is at the C-4 position (e.g., GYKI 52466) of the diazepine ring, the compounds bind to one site,[12,13] but if a carbonyl group is at the C-4 position, those compounds bind to another site.[11]

When 2,3-BDZ-11-2 and 2,3-BDZ-2 are compared (Figure 1), the only structural difference is that the 7,8-methylenedioxy moiety on 2,3-BDZ-2 is replaced with a 7,8-ethylenedioxy moiety as in 2,3-BDZ-11-2. This structural change results in a

dx.doi.org/10.1021/bi2017552 | Biochemistry 2012, 51, 1787−1795

change in the binding site. Furthermore, on the basis of inhibition constants (Table 1), 2,3-BDZ-11-2 is roughly as effective as 2,3-BDZ-2 in inhibiting the closed-channel state of GluA2Q$_{flip}$ [i.e., K_I values of 21 μM for 2,3-BDZ-11-2 and 25 μM for 2,3-BDZ-2 (Table 1)], but it is almost 5-fold less potent in inhibiting the open-channel state. Thus, the functional consequence of replacing the 7,8-methylenedioxy moiety on 2,3-BDZ-2 with the 7,8-ethylenedioxy moiety, yielding 2,3-BDZ-11-2, is a change of the binding site for 2,3-BDZ-11-2 but at a cost of the reduction of the potency. However, that reduction in potency for 2,3-BDZ-11-2, which is only for the open-channel state, turns it into a closed-channel-preferring inhibitor, unlike 2,3-BDZ-2.[11]

The results from this study show the presence of the 7,8-ethylenedioxy moiety on the diazepine ring (Figure 1) renders 2,3-BDZ-11-2 (and 2,3-BDZ-11-4) incapable of binding to either the 2,3-BDZ-2 site (Figure 7B) or the GYKI 52466 site (Figure 7C). In other words, if there is an additional change at the 7,8-position in the diazepine ring, the nature of the C-4 substitution is no longer the determinant of both the binding site and the conformational selectivity of the resulting compounds.[11−13] Our results suggest that the size of the ring at the 7,8-position seems to be a more critical "atomic descriptor" in that the increase in ring size from a five-membered to a six-membered ring (i.e., from dioxole to dioxane moiety) overrides the nature of the C-4 substitution. The impact of the increase in ring size from a dioxole to a dioxane moiety on the binding site for the resulting compounds might reflect the intimate molecular contact between the 7,8-position and the receptor site. Two interesting questions now arise. First, can the correlation between a change in the size of the dioxole ring and the binding site be extended beyond the ring enlargement from the dioxole to the dioxane moiety? Second, can modulation of the dioxole ring, i.e., the methylene group of the methylenedioxy function, be used as a novel method to explore undiscovered, noncompetitive binding sites? For example, the 7,8-methylenedioxy moiety can be replaced with 7,8-ethylidenedioxy or 7,8-isopropylidenedioxy moieties. Alternatively, a hydrogen atom on the 7,8-methylenedioxy moiety can be substituted with a chlorine atom to generate a different analogue. Such changes could produce new 2,3-BDZ analogues with different potencies, and these new analogues could also bind to new regulatory site(s) on the same receptor. In other words, these structural changes may allow us to find new sites for developing more potent and more selective 2,3-BDZ compounds.

Comparison of the Potency of 2,3-BDZ-11-2 of 2,3-BDZ-11-4. 2,3-BDZ-11-4 and 2,3-BDZ-11-2 bind to the same site because both have the 7,8-ethylenedioxy moiety on the diazepine ring. However 2,3-BDZ-11-4 is ∼10- and ∼3-fold stronger in inhibiting the closed- and open-channel states, respectively, than 2,3-BDZ-11-2. These results suggest that substitution of a hydrogen atom with a chlorine atom at C-3 on the aminophenyl ring increases the potency of the resulting compound, i.e., 2,3-BDZ-11-4, without changing the binding site or the mechanism of action or the conformational selectivity for the GluA2Q$_{flip}$ receptor. The higher potency of 2,3-BDZ-11-4 seems to be realized even at the first step involving the formation of the initial receptor−inhibitor intermediate, as judged by the inhibition constants for both the open- and closed-channel states between 2,3-BDZ-11-2 and 2,3-BDZ-11-4 (Figure 5 and Table 1). Specifically, the receptor−2,3-BDZ-11-4 intermediate formed in the closed-channel state is ∼4-fold more inhibitory than the receptor−2,3-BDZ-11-2 counterpart [i.e., K_I* = 9 μM for 2,3-BDZ-11-4 and 39 μM for 2,3-BDZ-11-2 (Table 1)]. Furthermore, the receptor−2,3-BDZ-11-4 intermediate formed in the open-channel state is 2-fold more inhibitory than the receptor−2,3-BDZ-11-2 intermediate [i.e., $\overline{K_I}$* of 24 μM for 2,3-BDZ-11-4 but 43 μM for 2,3-BDZ-11-2 (Table 1)]. This analysis suggests that new compounds that bind to this new site but with a potency higher than that of 2,3-BDZ-11-2 can be made. Previously, we reported that the N-3 position on the benzodiazepine ring is one place where acetylation can improve the potency of resulting compounds.[11−13] The aminophenyl ring is now the second place where chemical modifications can also improve the potency of the resulting compounds without changing the mechanism of action or the site of binding.

We do not know, however, whether the improved potency of the resulting compound, i.e., 2,3-BDZ-11-4, compared with that of 2,3-BDZ-11-2, is due to the addition of an electron-withdrawing group (i.e., chlorine atom) or other factors. If it is the former, the presence of an electron-withdrawing group on the aminophenyl ring could stabilize the interaction between the aminophenyl moiety of the 2,3-BDZ compound and the receptor site (or most likely a pocket that accommodates the aminophenyl ring). If this is the case, substitution of more hydrogen atoms on the aminophenyl ring with additional chlorine atoms or even other electron-withdrawing groups or moieties might yield even more potent 2,3-BDZ derivatives. Other factors, however, could also be involved in defining the potency of the resulting compounds and should also be explored. These factors include the shape and stereochemical arrangement of substitutions at the *ortho* position. It is important to note, however, that to construct better inhibitors, any new possibilities for generating chemical modifications at the *ortho* position must adhere to the 7,8-ethylenedioxy moiety on the diazepine ring in their structures, like 2,3-BDZ-11-4 or 2,3-BDZ-11-2. If new compounds were to bind to a different site, the predictions based on this unique feature of the structure−activity relationship will not be applicable.

In conclusion, we found that substituting the methylenedioxy with ethylenedioxy feature at the 7,8-position in the benzodiazepine ring is more critical than the C-4 substitution in determining the site of binding for the resulting compounds. As a result, the nature of the C-4 substitution as we reported earlier is only a dominant determinant of both the binding site and the conformational selectivity of 2,3-BDZ compounds with the 7,8-methylenedioxy moiety. A ring enlargement, at least from 7,8-methylenedioxy to 7,8-ethylenedioxy, then makes the resulting 2,3-BDZ compounds bind to an unique noncompetitive site, the third one we have reported thus far. The fact that a simple change in structure leads to a dramatic change in site may well reflect an intimate molecular contact between the 7,8-methylenedioxy ring and presumably a tight receptor pocket. We therefore speculate that chemical modifications of the 7,8-methylenedioxy ring, in addition to ring enlargement, lead to new compounds that may likely bind to new sites. Furthermore, for the 2,3-BDZ compounds with the 7,8-ethylenedioxy feature, chemical modifications of the 1-(4-aminophenyl) ring can improve the potency of the resulting compounds.

■ ASSOCIATED CONTENT

Supporting Information

Effect of 2,3-BDZ-11-2 on GluA2Q$_{flip}$ channel desensitization (Figure S1), its effect on k_{op} and k_{cl} (Figure S2), the A/A_I values as a function of 2,3-BDZ-11-2 concentration collected from the laser-pulse photolysis measurement (Figure S3) and

dx.doi.org/10.1021/bi2017552 | *Biochemistry* 2012, 51, 1787−1795

separately collected from a solution flow measurement (Figure S4), and the A/A_I values as a function of 2,3-BDZ-11-2 concentration on the flop isoform of GluA2Q (Figure S5). This material is available free of charge via the Internet at http://pubs.acs.org.

AUTHOR INFORMATION

Corresponding Author

*Telephone: (518) 591-8819. Fax: (518) 442-3462. E-mail: lniu@albany.edu.

Funding

This work was supported by grants from National Institute of Neurological Disorders and Stroke (R01 NS060812) and the Muscular Dystrophy Association (to L.N.).

Notes

The authors declare no competing financial interest.

ABBREVIATIONS

AMPA, α-amino-3-hydroxy-5-methyl-4-isoxazolepropionic acid; 2,3-BDZ, 2,3-benzodiazepine; GYKI 52466, 1-(4-aminophenyl)-4-methyl-7,8-methylenedioxy-5*H*-2,3-benzodiazepine; 2,3-BDZ-2, 1-(4-aminophenyl)-3,5-dihydro-7,8-methylenedioxy-2,3-benzodiazepin-4-one; 2,3-BDZ-11-2, 1-(4-aminophenyl)-3,5-dihydro-7,8-ethylenedioxy-4*H*-2,3-benzodiazepin-4-one; 2,3-BDZ-11-4, 1-(4-amino-3-chlorophenyl)-3,5-dihydro-7,8-ethylenedioxy-4*H*-2,3-benzodiazepin-4-one; HEK, human embryonic kidney.

REFERENCES

(1) Tarnawa, I., Farkas, S., Berzsenyi, P., Pataki, A., and Andrasi, F. (1989) Electrophysiological studies with a 2,3-benzodiazepine muscle relaxant: GYKI 52466. *Eur. J. Pharmacol. 167*, 193−199.

(2) Solyom, S., and Tarnawa, I. (2002) Non-competitive AMPA antagonists of 2,3-benzodiazepine type. *Curr. Pharm. Des. 8*, 913−939.

(3) Micale, N., Colleoni, S., Postorino, G., Pellicanò, A., Zappalà, M., Lazzaro, J., Diana, V., Cagnotto, A., Mennini, T., and Grasso, S. (2008) Structure-activity study of 2,3-benzodiazepin-4-ones noncompetitive AMPAR antagonists: Identification of the 1-(4-amino-3-methylphenyl)-3,5-dihydro-7,8-ethylenedioxy-4H-2,3-benzodiazepin-4-one as neuroprotective agent. *Bioorg. Med. Chem. 16*, 2200−2211.

(4) Zappalà, M., Pellicanò, A., Micale, N., Menniti, F. S., Ferreri, G., De Sarro, G., Grasso, S., and De Micheli, C. (2006) New 7,8-ethylenedioxy-2,3-benzodiazepines as noncompetitive AMPA receptor antagonists. *Bioorg. Med. Chem. Lett. 16*, 167−170.

(5) Dingledine, R., Borges, K., Bowie, D., and Traynelis, S. F. (1999) The glutamate receptor ion channels. *Pharmacol. Rev. 51*, 7−61.

(6) Palmer, C. L., Cotton, L., and Henley, J. M. (2005) The molecular pharmacology and cell biology of α-amino-3-hydroxy-5-methyl-4-isoxazolepropionic acid receptors. *Pharmacol. Rev. 57*, 253−277.

(7) Rogawski, M. A. (2011) Revisiting AMPA receptors as an antiepileptic drug target. *Epilepsy Curr. 11*, 56−63.

(8) Donevan, S. D., and Rogawski, M. A. (1993) GYKI 52466, a 2,3-benzodiazepine, is a highly selective, noncompetitive antagonist of AMPA/kainate receptor responses. *Neuron 10*, 51−59.

(9) Rammes, G., Swandulla, D., Collingridge, G. L., Hartmann, S., and Parsons, C. G. (1996) Interactions of 2,3-benzodiazepines and cyclothiazide at AMPA receptors: Patch clamp recordings in cultured neurones and area CA1 in hippocampal slices. *Br. J. Pharmacol. 117*, 1209−1221.

(10) Li, G., and Niu, L. (2004) How fast does the GluR1Qflip channel open? *J. Biol. Chem. 279*, 3990−3997.

(11) Ritz, M., Micale, N., Grasso, S., and Niu, L. (2008) Mechanism of inhibition of the GluR2 AMPA receptor channel opening by 2,3-benzodiazepine derivatives. *Biochemistry 47*, 1061−1069.

(12) Ritz, M., Wang, C., Micale, N., Ettari, R., and Niu, L. (2011) Mechanism of Inhibition of the GluA2 AMPA Receptor Channel Opening: The Role of 4-Methyl versus 4-Carbonyl Group on the Diazepine Ring of 2,3-Benzodiazepine Derivatives. *ACS Chem. Neurosci. 2*, 506−513.

(13) Wang, C., Sheng, Z., and Niu, L. (2011) Mechanism of Inhibition of the GluA2 AMPA Receptor Channel Opening: Consequences of Adding an N-3 Methylcarbamoyl Group to the Diazepine Ring of 2,3-Benzodiazepine Derivatives. *Biochemistry 50*, 7284−7293.

(14) Kawahara, Y., Ito, K., Sun, H., Aizawa, H., Kanazawa, I., and Kwak, S. (2004) Glutamate receptors: RNA editing and death of motor neurons. *Nature 427*, 801.

(15) Sommer, B., Kohler, M., Sprengel, R., and Seeburg, P. H. (1991) RNA editing in brain controls a determinant of ion flow in glutamate-gated channels. *Cell 67*, 11−19.

(16) Liu, S. J., and Zukin, R. S. (2007) Ca^{2+}-permeable AMPA receptors in synaptic plasticity and neuronal death. *Trends Neurosci. 30*, 126−134.

(17) Li, G., Pei, W., and Niu, L. (2003) Channel-opening kinetics of $GluR2Q_{flip}$ AMPA receptor: A laser-pulse photolysis study. *Biochemistry 42*, 12358−12366.

(18) Huang, Z., Li, G., Pei, W., Sosa, L. A., and Niu, L. (2005) Enhancing protein expression in single HEK 293 cells. *J. Neurosci. Methods 142*, 159−166.

(19) Papageorgiou, G., Lukeman, M., Wan, P., and Corrie, J. E. (2004) An antenna triplet sensitiser for 1-acyl-7-nitroindolines improves the efficiency of carboxylic acid photorelease. *Photochem. Photobiol. Sci. 3*, 366−373.

(20) Udgaonkar, J. B., and Hess, G. P. (1987) Chemical kinetic measurements of a mammalian acetylcholine receptor by a fast-reaction technique. *Proc. Natl. Acad. Sci. U.S.A. 84*, 8758−8762.

(21) Pei, W., Huang, Z., Wang, C., Han, Y., Park, J. S., and Niu, L. (2009) Flip and flop: A molecular determinant for AMPA receptor channel opening. *Biochemistry 48*, 3767−3777.

(22) Tolle, T. R., Berthele, A., Zieglgansberger, W., Seeburg, P. H., and Wisden, W. (1995) Flip and Flop variants of AMPA receptors in the rat lumbar spinal cord. *Eur. J. Neurosci. 7*, 1414−1419.

(23) Pei, W., Huang, Z., and Niu, L. (2007) GluR3 flip and flop: Differences in channel opening kinetics. *Biochemistry 46*, 2027−2036.

(24) Lodge, D., Bond, A., O'Neill, M. J., Hicks, C. A., and Jones, M. G. (1996) Stereoselective effects of 2,3-benzodiazepines in vivo: Electrophysiology and neuroprotection studies. *Neuropharmacology 35*, 1681−1688.

(25) Bleakman, D., Ballyk, B. A., Schoepp, D. D., Palmer, A. J., Bath, C. P., Sharpe, E. F., Woolley, M. L., Bufton, H. R., Kamboj, R. K., Tarnawa, I., and Lodge, D. (1996) Activity of 2,3-benzodiazepines at native rat and recombinant human glutamate receptors in vitro: Stereospecificity and selectivity profiles. *Neuropharmacology 35*, 1689−1702.